



KAROLINSKA INSTITUTET  
TECHNICAL AUDIOLOGY

Report TA129

Dec 1993

**Time-frequency signal representation of transient evoked  
otoacoustic emissions via smoothed pseudo Wigner  
distribution**

*Jun Cheng*



## **Time-frequency signal representation of transient evoked otoacoustic emissions via smoothed pseudo Wigner distribution**

Jun Cheng

### **ABSTRACT**

The smoothed pseudo Wigner distribution (SPWD) can be used to process transient evoked otoacoustic emissions (TEOAEs). By this process emissions patterns can be shown in the time-frequency plane with better time and frequency resolution than in a conventional spectrogram. Such analyses of shape and localization of TEOAEs patterns and comparisons of patterns obtained at different physiological or pathological situations, open a new way to describe otoacoustic emissions. Better understanding and interpreting of the characteristics of TEOAEs can be achieved as well. This method can be used as a powerful tool to monitor the cochlear condition. Pilot investigations are demonstrated.

**Keywords:** evoked otoacoustic emissions, time-frequency representation, Wigner distribution, spectrogram

*This work was supported by the Swedish Council for Social Research (SFR).*

---

*Mailing address:*  
Teknisk Audiologi / KI  
Box 70025  
S-100 44 STOCKHOLM  
Sweden

*Visiting address:*  
Teknisk Audiologi  
Lindstedtsvägen 7  
Kgl. Tekniska Högskolan  
Stockholm

*Telephone:*  
Nat.: 08-411 66 60  
Int.: +46 8 411 66 60

*Fax:*  
Nat.: 08-791 71 30  
Int.: +46 8 791 71 30

CONTENTS	page
INTRODUCTION.....	1
MATERIAL AND METHODS.....	4
RESULTS.....	6
DISCUSSION.....	10
CONCLUSIONS.....	12
ACKNOWLEDGEMENTS.....	12
REFERENCES.....	12
APPENDIX A.....	16
APPENDIX B.....	17

## INTRODUCTION

Otoacoustic emissions (OAEs) are acoustic energy measured in the external ear canal. They originate within the cochlea and are normal by-products of the active process in hearing (Kemp, 1978; Gold, 1948). Several mechanisms have been proposed to be responsible for this process:

- a) Nonlinear motions of the basilar membrane, including active nonlinear processes which add energy to the motion of the basilar membrane; and passive nonlinear processes e.g. by compressive limiting and/or suggested unsymmetrically moving waves on the basilar membrane (Davis, 1983; Allen & Neely, 1992; Brass & Kemp, 1993a).
- b) A motile response of outer hair cells (OHC), which includes volume and length changes in the hair cells. These changes are frequency specific (Flock et al., 1986; Brundin et al., 1989).

There are two categories of OAEs, spontaneous and evoked OAEs. Spontaneous OAEs (SOAEs) are tonal, low level emissions, which are produced without acoustic stimulation. They appear in about 60-70% of normal hearing ears (Martin et al., 1990; Zwicker, 1990). SOAEs indicate that the ear uses active feedback to limit the amplitude of the internal oscillation to small inaudible values. OAEs can be evoked in almost all normal hearing ears. These emissions are classified into three subgroups by the stimuli used to evoke them: transient evoked OAEs (TEOAEs), stimulus-frequency OAEs (SFOAEs) and distortion-product OAEs (DPOAEs). TEOAEs occur after brief stimuli (Kemp, 1978), e.g. clicks. They are sometimes referred to as delayed evoked otoacoustic emissions (DEOAEs) (Zwicker, 1983) or click-evoked otoacoustic emissions (CEOAEs) (Johnsen et al., 1993). SFOAEs are elicited by long-duration tones, and occur at the stimulus frequency (Brass & Kemp, 1993b). DPOAEs are produced by stimulation with two primary tones at frequencies of  $f_1$  and  $f_2$  ( $f_1 < f_2$ ), and occur e.g. at the frequency  $2f_1 - f_2$  (Harris et al., 1987), corresponding to the cubic distortion tone with its frequency below the primary frequencies. DPOAEs are very sensitive to the amount of separation of the primary tones.

The cochlear sensitivity and dynamic range can be studied by measuring amplitude growth of the TEOAEs as a function of stimulus level (Norton, 1993). In the normal-hearing ear, at low stimulus levels, the amplitude of the TEOAEs increases as the stimulus level is increased. When the stimulus level approaches 50-60 dB SPL, the amplitude of the TEOAEs increases more slowly and finally saturates. In the impaired ear, TEOAEs begin to appear at higher levels, and the growth rates are higher in an ear with a smaller dynamic range.

Since TEOAEs can be measured objectively and non-invasively by a probe including a microphone and a receiver sealed in the ear canal, they are potentially powerful for screening purposes, especially for neonates and young children (Bray and Kemp, 1987). TEOAE measurements also have good reproducibility in both time and frequency domain even if the measurements are weeks apart (Norton, 1993). In another investigation, the amplitude of TEOAEs was stable over successive short-term measurements, with a variability within individual spectral bands of approximately 1 dB from 0.9 to 4.1 kHz (Harris et al., 1991). Since TEOAEs have the same contents over time, they can be used as a sensitive indicator to monitor the cochlear function and the frequency sensitivity of the inner ear.

In this paper, the influence of hearing loss on the TEOAEs is discussed. Kemp et al. (Kemp et al., 1990a) suggested that there are relations between audiograms and TEOAEs, and that TEOAEs can be used to identify frequency ranges of normal hearing in pathological ears. In various studies TEOAEs were never found when the hearing loss at the best frequency was worse than 40 dB HL (Collet et al., 1993a; Collet et al., 1993b). Furthermore, when pure-tone averages (PTA; 1000, 2000 and 4000 Hz) were greater than 40 dB HL, TEOAEs were never observed in response to 86 dB SPL clicks (Norton, 1993). In ears with sloping hearing losses (Johnsen et al., 1993) the thresholds at 1 and 2 kHz were most important for the presence of TEOAEs.

The TEOAEs consist of a large number of individual components which overlap both in the time and in the frequency domain. After stimulations, high frequency emissions have shorter latency, since they originate from the basal portion in cochlea, whereas low frequency emissions have longer latency, since they originate from the apical portion in the cochlea. The analysis is difficult by

using one-dimensional methods i.e. to get time or frequency representations. TEOAEs can be transformed into the time-frequency plane in time-frequency representations (TFRs) and give a three-dimensional pattern, in which individual frequency components and times of their arrival could be identified.

The most common way to obtain the TFRs is based on the short-time Fourier transform (STFT) and a sliding analysis window (Hlawatsch & Boudreaux-Bartels, 1992). The result is usually called "spectrogram". The STFT (and the spectrogram) are defined as

$$STFT_x^{(\gamma)}(t, f) = \int_t [x(t') \gamma(t' - t)] e^{-j2\pi f t'} dt'$$

$$SPEC_x^{(\gamma)}(t, f) = |STFT_x^{(\gamma)}(t, f)|^2$$

where  $x(t)$  is the signal,  $t$  and  $f$  denote time and frequency respectively,  $\gamma(t)$  is the analysis window, and the integrations are performed from  $-\infty$  to  $\infty$ . The signal is assumed to be stationary within the specific analysis window. So STFT is a "local spectrum" of the signal at the time  $t$ . SPEC is the spectrogram of the signal. The resolution in time and the resolution in frequency are related in the spectrogram. A good time resolution requires a short window, which will give bad frequency resolution, and vice versa.

The Wigner distribution (WD) (Wigner, 1932) has been used as a powerful tool to analyze time-varying systems and non-stationary signals (Claasen & Mecklenbräuker, 1980; Smits, 1992). In practice, discrete-time and smoothing versions are used to overcome interference terms (ITs) in digital signal processing (Sessarego et al, 1989; Krattenthaler & Hlawatsch, 1993). WD and its smoothed version SPWD (smoothed pseudo WD) are given by

$$D_x(t, f) = \int_{\tau} x(t + \frac{\tau}{2}) x^*(t - \frac{\tau}{2}) e^{-j2\pi f \tau} d\tau$$

$$SPWD_x^{(g,\eta)}(t, f) = \int_{\tau} \left[ \int_{t'} g(t-t') x(t'+\frac{\tau}{2}) x^*(t'-\frac{\tau}{2}) dt' \right] \cdot \eta(\frac{\tau}{2}) \eta^*(-\frac{\tau}{2}) e^{-j2\pi f \tau} d\tau$$

in which  $g(t)$  and  $\eta(t)$  are two windows whose effective lengths independently determine the time smoothing and the frequency smoothing,  $t$  and  $f$  denote time and frequency respectively, the superscript  $*$  denotes complex conjugation, and the integrations are performed from  $-\infty$  to  $\infty$ . The discrete version of SPWD is defined in Appendix A.

The aim of this study was to investigate potentially interesting relations between TEOAEs and its TFRs using SPWD, and to evaluate the cochlear condition by inspection of distribution patterns of the emissions. It would be interesting to see if such distribution patterns could map the cochlear activity along the basilar membrane.

## MATERIAL AND METHODS

TEOAEs were measured with a digital signal processing system (DSP) consisting of a TMS32010 signal processor, 12 bits AD/DA converters, tracking anti-aliasing filters, program controllable attenuator and preamplifier. A separate preamplifier was used instead of program controllable preamplifier to get higher gain when needed. B-type probes (Otodynamics Ltd) were used, which were originally designed for the ILO88 and ILO92 (Otodynamics Ltd) systems. The DSP system was controlled by a IBM compatible personal computer (PC). Software for the TEOAE recording was written for both DSP system and PC in assembly and high level programming language. The SPWD program runs under PC's environment. TFRs curves can be printed out to a black & white laser printer or a colour printer (HP DeskJet 550C).

In accordance with the ILO88 system (Kemp et al., 1990b) 80  $\mu$ s nonfiltered click stimuli drive the receiver in the probe which is sealed in the ear canal.

Responses from 1000 sweeps are averaged in the time domain to reduce the effect of noise. In the linear mode all the clicks have the same level and the same polarity. In the nonlinear mode, the fourth click in every group of four clicks has reversed polarity and the level is increased by a factor of 3. In the nonlinear mode the responses to all linearly behaving parts of the system are cancelled by summation of responses; only the nonlinear part of the emissions can be left which represents physiological activity in the cochlea. To remove the primary stimulus artifact in the recorded TEOAE response a window is used. It is zero from 0 to 2.5 ms, it is cosine raised from 2.5 to 5 ms, it is unity from 5 to 18 ms and finally, it is cosine faded from 18 to 20.5 ms. Two separate records were carried out. The sampling frequency was 25 kHz. The peak-equivalent stimulus level in the ear canal was calibrated on an artificial head (Kemar) with type 4257 ear simulator, type 2607 measurement amplifier (Brüel & Kjær).

To test the SPWD algorithm and to simulate the "chirp" effect of the TEOAEs, two "crossed" linear FM signals (chirp signals) were used as algorithm input signal:

$$x(t) = \cos[125000(2\pi)t^2] + \cos[125000(2\pi)(0.02-t)^2].$$

The first part has an instantaneous frequency of

$$f(t) = 250000t \text{ Hz.}$$

The second part has an instantaneous frequency of

$$f(t) = 5000 - 250000t \text{ Hz.}$$

$t$  and  $f$  denote time (second) and frequency (Hz) respectively. In Fig. 1 the performance of SPWD and spectrogram for the algorithm input signal and for the TEOAEs are demonstrated. The time-frequency resolution in the SPWD is higher than in the spectrogram, and the power is more concentrated in the SPWD.



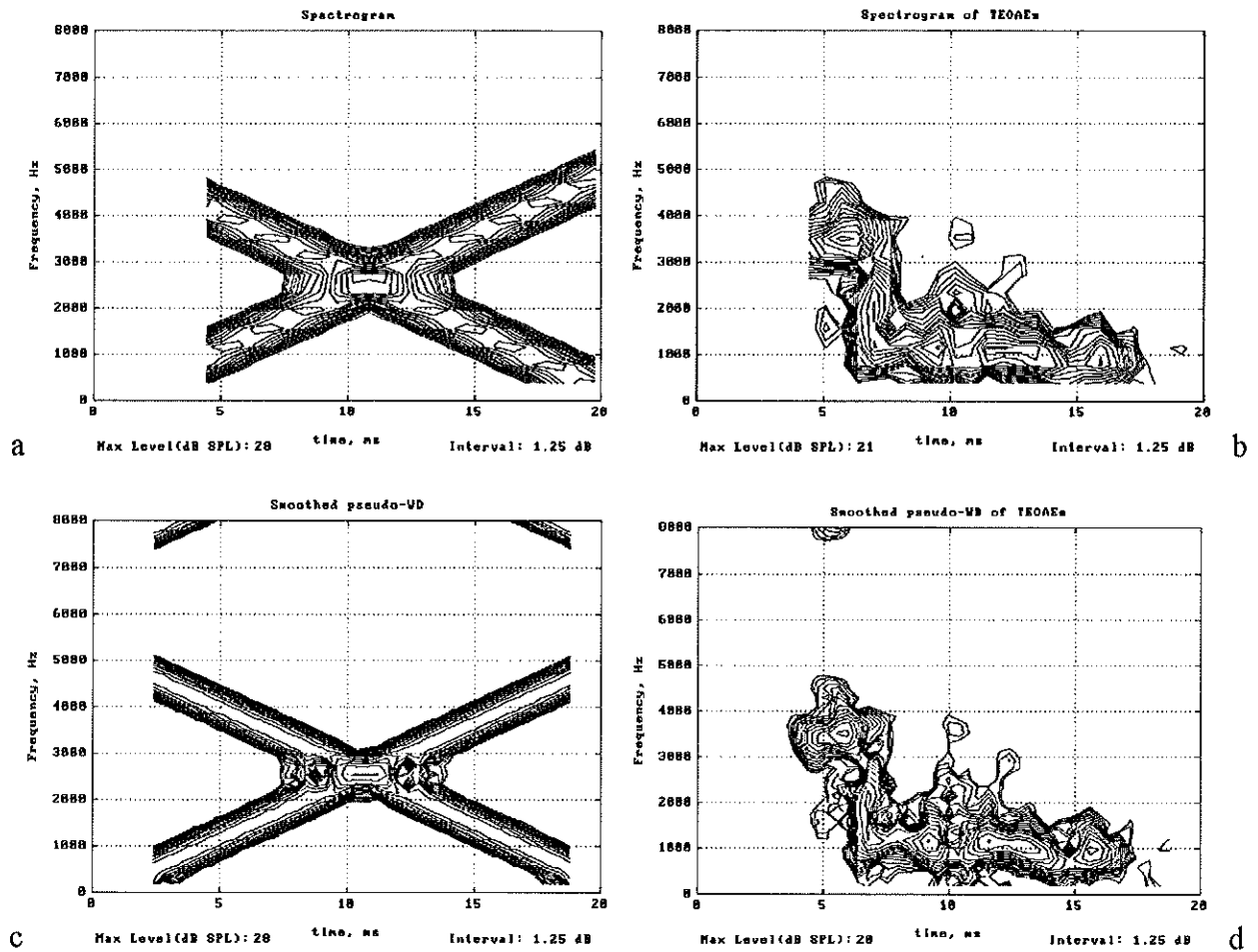


Fig. 1. SPWD and spectrogram for algorithm input signal and for TEOAEs. a. Spectrogram of input signal. b. Spectrogram of TEOAEs. c. SPWD of input signal. d. SPWD of TEOAEs.

## RESULTS

Fig. 2 shows an example of TEOAEs at nonlinear mode and its SPWDs at different stimulus levels (75, 85, 95 and 105 dB SPL) for a certain normal ear. In left panels of Fig. 2a-d the top left curves show the averaged stimulus in the external ear canal and the window function. The lower curves show TEOAEs of two consecutive measurements. The top right curves show the spectrum of the TEOAEs defined as the cross-power spectrum of two responses and the noise spectrum defined as the power spectrum of the difference of two

responses in lower curves. In right panels of Fig.2a-d the lower curves show the average of two consecutive responses. The left curves show the corresponding power spectrum. The maximum amplitudes of the TEOAEs on SPWDs are 18, 20, 27 and 30 dB in response to 75, 85, 95 and 105 dB SPL stimulus levels. However, the emission pattern and localization are unchanged. The amplitude of the TEOAEs grows nonlinearly with stimulus level. At the lower stimulus level, 75 dB SPL, Fig.2a, the measured TEOAEs have a lower signal-to-noise-ratio. Then the amplitude of TEOAEs increases as the stimulus level is increased (Fig.2b and Fig.2c). Finally the amplitude of the TEOAEs is about saturated (Fig.2d) at about 30 dB in response to a 105 dB SPL stimulus.

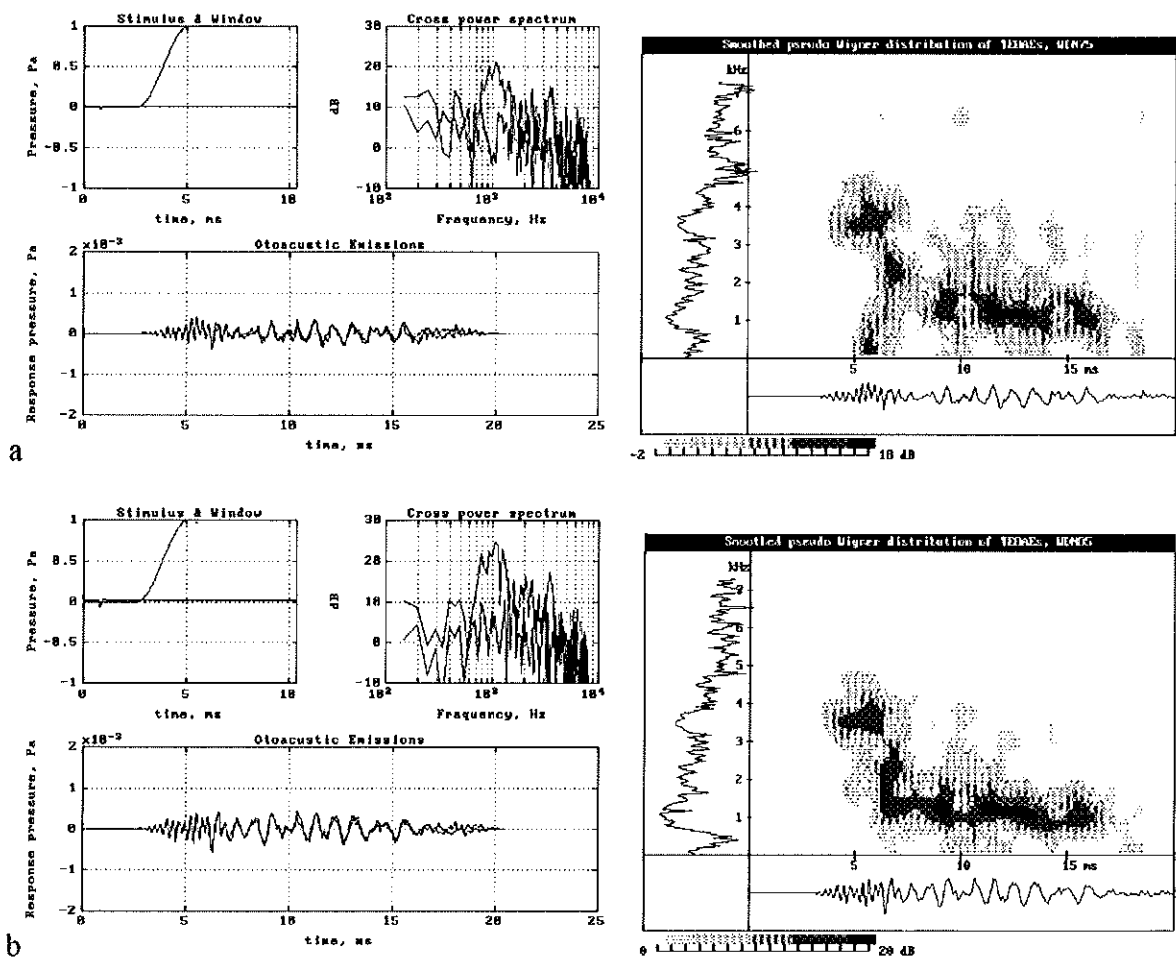


Fig.2 (continued on the next page, with legend).

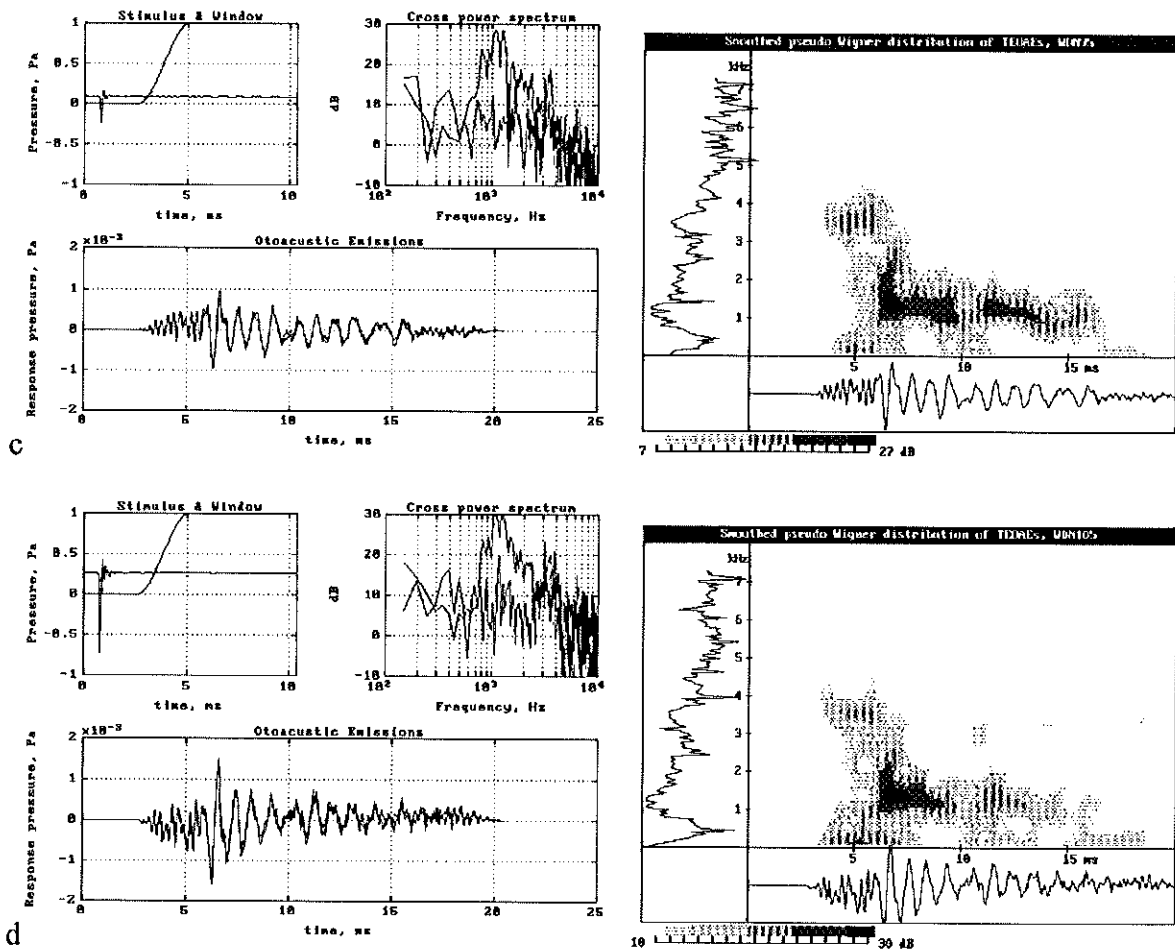


Fig.2. Nonlinear TEOAEs and its SPWD of one ear. Data from one adult subject in response to four different stimulus levels. a. 75 dB SPL. b. 85 dB SPL. c. 95 dB SPL. d. 105 dB SPL.

Fig.3 shows another example of two SPWDs of nonlinear TEOAEs from one neonate.

To separate the TEOAEs from artifacts, SPWD is an effective method. Fig.4 shows SPWD of TEOAEs of same ear at the same stimulus level for the linear and nonlinear stimulus modes. Artifacts can be identified by comparing SPWDs. In Fig.4a TEOAEs at linear mode SPWD has an extra peak at about 4.5 ms and 1.8 kHz, which is corresponding to the artifact. This peak does not exist at all on the SPWD of the TEOAEs in the nonlinear mode in Fig.4b.

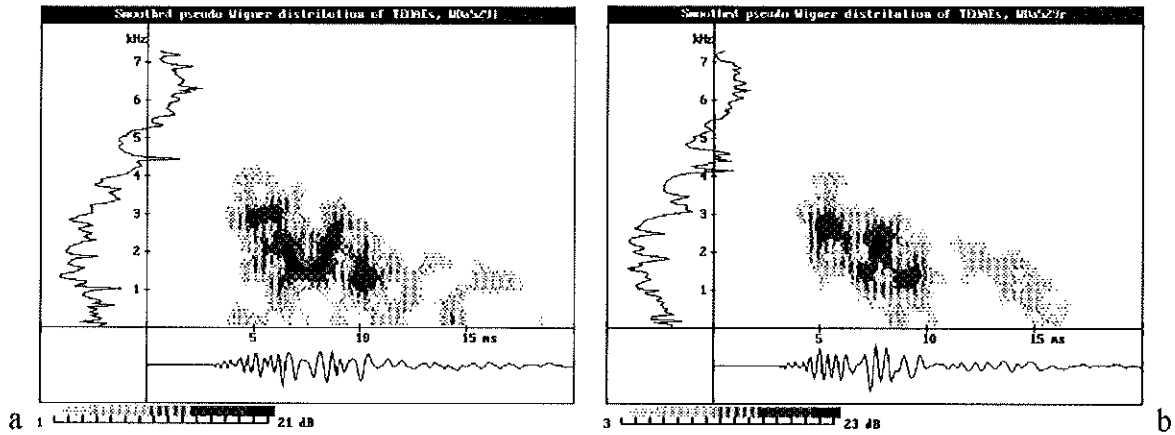


Fig.3. SPWDs of TEOAEs from one neonate. a. Left ear. b. Right ear

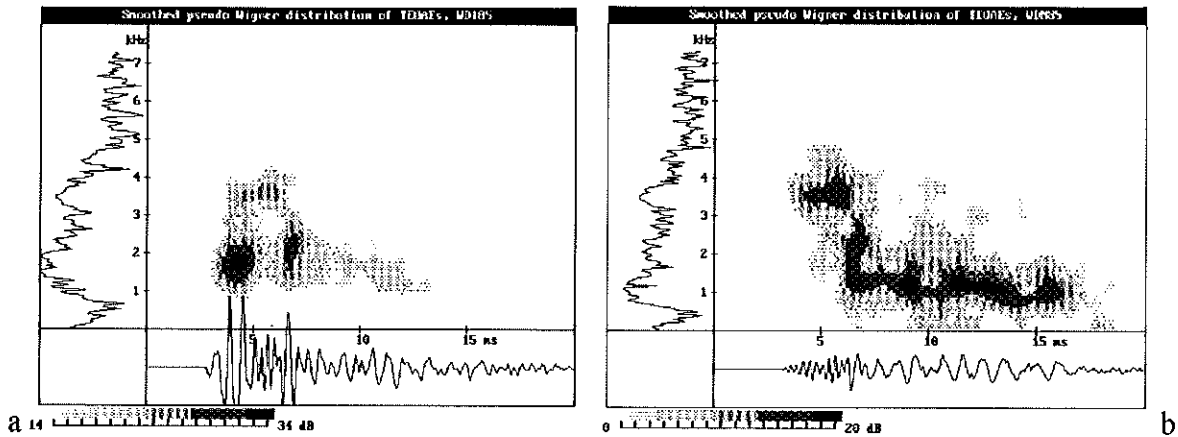


Fig.4. SPWDs of TEOAEs in linear and nonlinear modes. a. Linear. b. Nonlinear.

In Fig.5, the main panel shows the averaged SPWD of the TEOAEs in nonlinear mode from 54 neonatal ears. From this averaged SPWD of TEOAEs we can estimate the existence of various frequency components and times of arrival. We can use this averaged SPWD as a map of the averaged cochlear

activity along the basilar membrane. By comparison with the SPWD of an individual ear it is possible to comment on the cochlear conditions of a neonate.

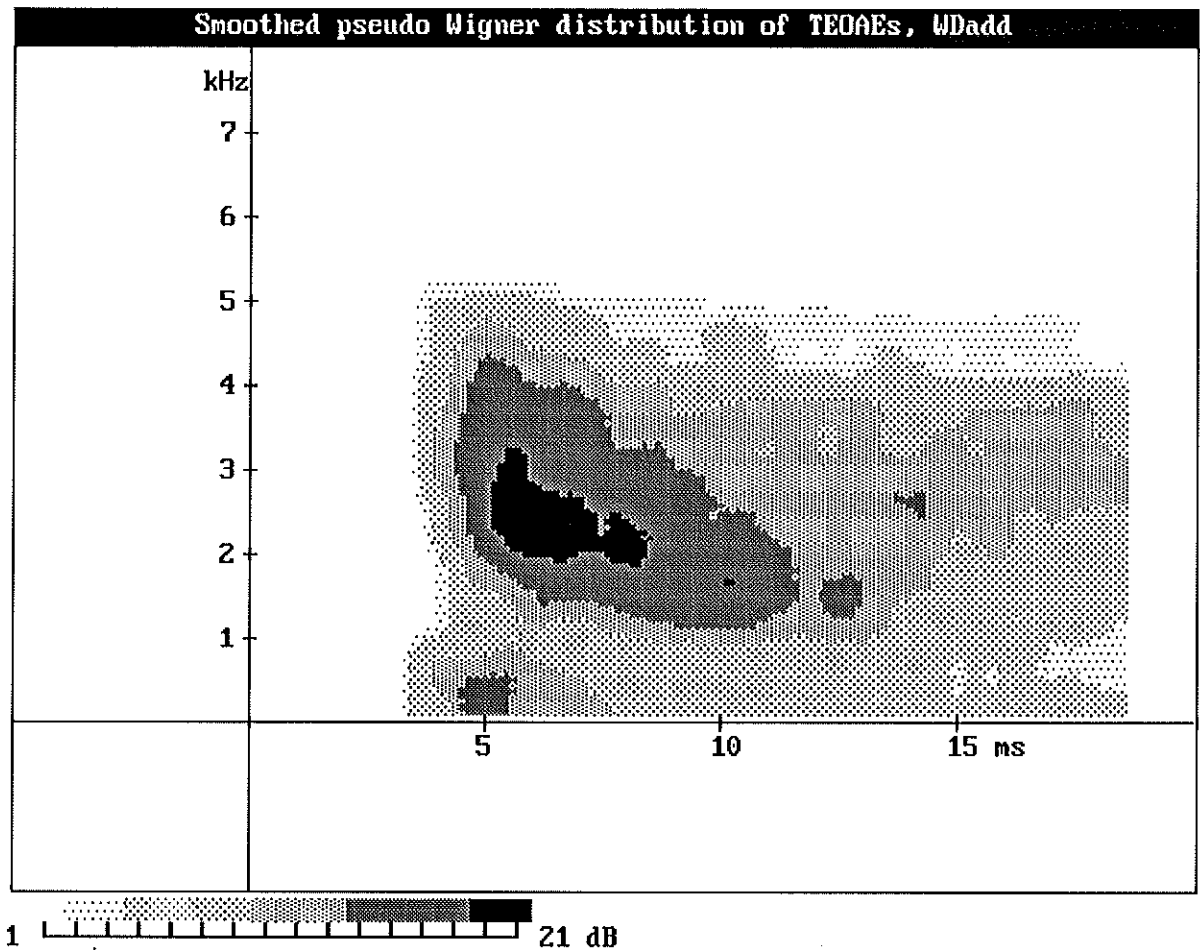


Fig.5. Averaged SPWD of TEOAEs from 54 neonatal ears.

## DISCUSSION

In the spectrogram analysis method based on STFT, it is assumed that the signal is stationary within a specific analysis window. Shorter window length is limited by frequency resolution. When the spectral content changes rapidly over

time, like for TEOAEs, an accurate estimate is impossible. Using SPWD is an effective way to meet this problem.

With the ILO88 system, the power spectrum consists of about 200 Hz wide bins from 0.5 to 5.3 kHz (Kemp et al., 1990b). With the SPWD better performance can be achieved. The SPWD also gives information regarding response delay and frequency contents.

Using the WD algorithm, it should be noted that the sampling frequency must be more than twice the Nyquist frequency to avoid aliasing problems. An unaliased WD algorithm was proposed (Bekir, 1993).

Time averaging and delay criterion technique is used to extract TEOAEs from noise. The traditional technique to extract evoked signals from noise relies on: a) The evoked signal to a specific stimulus is time-invariant. b) Signal and noise are uncorrelated. c) Signal and noise are additive. (see Appendix B for detail.) In the measurement all signals, except TEOAEs, are treated as noise. For example, SOAEs are treated as noise as long as they are not synchronous to and time locking with stimulations. In that case SOAEs are cancelled away by the time averaging procedure. If SOAEs are synchronous to and time locking with stimulation they will be presented as horizontal bars on the SPWD.

Recently, a study on prediction of hearing susceptibility to the damaging effects of noise by inspection of TEOAEs was carried out (Hotz et al., 1993). It was shown that the response amplitudes of the TEOAEs in the frequency domain may be significantly changed in the range from 2 to 4 kHz after broadband noise exposure. This method seemed more sensitive than pure-tone audiometry in detecting early cochlear damage from noise. The SPWD algorithm might also be used in this kind of studies. The noise induced TEOAE changes can be evaluated both in the time and in the frequency domain by analysing the differences with the SPWD of the TEOAEs after noise exposure. This method might be more feasible as a screening procedure for measuring hearing susceptibility to noise exposure than pure-tone audiometry.

## CONCLUSIONS

SPWD can be used to process TEOAEs, and TEOAEs patterns can be shown in the time-frequency plane with better time and frequency resolution than in a conventional spectrogram. Better understanding and interpreting of the characteristics of TEOAEs and cochlear condition can be achieved by inspection of distribution patterns of the TEOAEs. The distribution pattern could map the cochlear activity along the basilar membrane.

## ACKNOWLEDGEMENTS

Some of TEOAEs recordings were kindly supplied by Mark E Lutman, Institute of Hearing Research, Audiology Centre, General Hospital, Nottingham, England.

The author would like to thank Åke Olofsson for the many valuable suggestions and discussions, his contributions were the essential to this work. Many thanks to Björn Hagerman and Ann-Cathrine Lindblad for the support and helpful comments to this manuscript, they made this work possible.

This work was supported by the Swedish Council for Social Research (SFR).

## REFERENCES

- Allen JB, Neely ST. Cochlear micromechanics. *Phys Today* 1992; 45: 40-47.
- Bekir EC. A contribution to the unaliased discrete-time Wigner distribution. *J Acoust Soc Am* 1993; 93: 363-371.
- Brass D, Kemp DT. Analyses of Mössbauer mechanical measurements indicate that the cochlea is mechanically active. *J Acoust Soc Am* 1993a; 93: 1502-1515.

- Brass D, and Kemp DT. Suppression of stimulus frequency otoacoustic emissions. *J Acoust Soc Am* 1993b; 93: 920-939.
- Bray P, and Kemp DT. An advanced cochlear echo technique suitable for infant screening. *Br J Audiol* 1987; 21: 191-204.
- Brundin L, Flock Å, Canlon B. Sound-induced motility of isolated cochlear outer cells is frequency-specific. *Nature* 1989; 342: 814-816.
- Claasen TACM, Mecklenbräuker WFG. The Wigner distribution - a tool for time-frequency signal analysis, Part I-III. *Philips J Res* 1980; 35: 217-250,276-300,372-389.
- Collet L, Levy V, Veuille E, Truy E, Morgon A. Click-evoked otoacoustic emissions and hearing threshold in sensorineural hearing loss. *Ear Hear* 1993a; 14: 141-143.
- Collet L, Veuille E, Chanal JM, Morgon A. Evoked otoacoustic emissions: correlates between spectrum analysis and audiogram. *Audiology* 1993b; 30: 164-172.
- Davis H. An active process in cochlear mechanics. *Hear Res* 1983; 9: 79-90.
- Flock Å, Flock B, Ulfendahl M. Mechanisms of movement in outer hair cells and possible structural basis. *Arch Otorhinolaryngol* 1986; 243: 83-89.
- Gold T. Hearing II. The physical basis of the action of cochlea. *Proc R Soc B* 1948; 135: 492-498.
- Harris FP, Stagner BB, Martin GK, Lonsbury-Martin BL. Effects of frequency separation of primary tones on the amplitude of acoustic distortion products. *J Acoust Soc Am* 1987; 82(Suppl 1): 117.
- Harris FP, Probst R, Wenger R. Repeatability of transiently evoked otoacoustic emissions in normally hearing humans. *Audiology* 1991; 30: 135-141.
- Hlawatsch F, Boudreaux-Bartels GF. Linear and quadratic time-frequency signal representations. *IEEE SP Magazine* april 1992; 21-67.



Hotz MA, Probst R, Harris FP, and Hauser R. Monitoring the effect of noise exposure using transiently evoked otoacoustic emissions. *Acta Otolaryngol* 1993; 113: 478-482.

Johnsen NJ, Parbo J, Elberling C. Evoked acoustic emissions from the human ear. VI. Findings in cochlear hearing impairment. *Scand Audiol* 1993; 22:87-95.

Kemp DT. Stimulated acoustic emissions from within the human auditory system. *J Acoust Soc Am* 1978; 64: 1386-1391.

Kemp DT, Ryan S, Bray P. Otoacoustic emission analysis and interpretation for clinical purposes. In F. Grandori, G. Gianfrone, and D.T. Kemp (eds): *Cochlear mechanisms and otoacoustic emissions*. *Adv Audiol*, Basel, Karger, 1990a: 7: 77-98.

Kemp DT, Ryan S, Bray P. A guide to the effective use of otoacoustic emissions. *Ear Hear* 1990b; 11: 93-105.

Krattenthaler W, Hlawatsch F. Time frequency design and processing of signals via smoothed Wigner distributions. *IEEE Trans Signal Processing* 1993; 41: 278-287.

Martin GK, Probst R, Lonsbury-Martin BL. Otoacoustic emissions in human ears: Normative findings. *Ear Hear* 1990; 11: 47-61.

Norton SJ. Application of transient evoked otoacoustic emission to pediatric populations. *Ear Hear* 1993; 14: 64-73.

Sessarego JP, Sageloli J, Flandrin P, Zakharia M. Time-frequency analysis of signals related to scattering problem in acoustics. Part I: Wigner-Ville analysis of echoes scattered by a spherical shell. In J.M. Combes, et al (eds): *Wavelet. Time-frequency methods and phase space*. Springer-Verlag, Berlin, 1989; 147-153.

Smits RLHM. Accuracy of spectrographic analysis of rapidly varying formants. *IPO Annual Progress Report* 1992; 27: 29-37.

Wigner EP. On the Quantum correction for thermodynamic equilibrium. *Phys Rev* 1932; 40: 749-759.

Zwicker E. Delayed evoked oto-acoustic emissions and their suppression by Gaussian shaped pressure impulses. *Hear Res* 1983; 11: 359-371.

Zwicker E. Otoacoustic emissions in research of inner ear signal processing. In F. Grandori, G. Gianfrone, and D.T. Kemp (eds): *Cochlear mechanisms and otoacoustic emissions*. *Adv Audiol*, Basel, Karger, 1990; 7: 63-76.

## APPENDIX A

The discrete-time version of SPWD come from the SPWD definition:

$$SPWD_x^{(g,\eta)}(t, f) = \int_{\tau} \left[ \int_{t'} g(t-t') x(t'+\frac{\tau}{2}) x^*(t'-\frac{\tau}{2}) dt' \right] \cdot \eta(\frac{\tau}{2}) \eta^*(-\frac{\tau}{2}) e^{-j2\pi f \tau} d\tau.$$

If  $\eta(t) = \eta(-t)$  and  $\tau' = \tau/2$ , then

$$SPWD_x^{(g,\eta)}(t, f) = 2 \int_{\tau'} \left[ \int_{t'} g(t-t') x(t'+\tau') x^*(t'-\tau') dt' \right] \cdot |\eta(\tau')|^2 e^{-j4\pi f \tau'} d\tau'.$$

If  $t'=t+m$ ,  $n=\tau'$ ,  $-M+1 < m < M-1$ ,  $-N+1 < n < N-1$ , then

$$SPWD_x^{(g,\eta)}(t, f) = 2 \sum_{n=-N+1}^{N-1} \left[ \sum_{m=-M+1}^{M-1} g(m) x(t+m+n) x^*(t+m-n) \right] \cdot |\eta(n)|^2 e^{-j4\pi f n}.$$

Let  $K_m(t, n) = \sum_{m=-M+1}^{M-1} g(m) x(t+m+n) x^*(t+m-n)$ ,  $\nu = 2f$ , then

$$SPWD_x^{(g,\eta)}(t, \nu) = 2 \sum_{n=-N+1}^{N-1} |\eta(n)|^2 K_m(t, n) e^{-j2\pi \nu n}.$$

This formulation is convenient for numerical implementation via fast Fourier transform (FFT) algorithms. In practice, a sliding analysis window is used for a short-time SPWD.

## APPENDIX B

Assessment of evoked signals by synchronous time averaging technique:

If the measured signals are  $x_i(n)$ , and the evoked signals are  $s_i(n)$  and the noise signals are  $\eta_i(n)$ , then

$$x_i(n) = s_i(n) + \eta_i(n).$$

After M times averaging

$$\frac{1}{M} \sum_{i=1}^M x_i(n) = \frac{1}{M} \sum_{i=1}^M s_i(n) + \frac{1}{M} \sum_{i=1}^M \eta_i(n).$$

If the evoked signals to a specific stimulus is time-invariant i.e.

$$s_1(n) = s_2(n) = \dots = s(n).$$

The noise signals variance  $\sigma_{\eta}^2 = \sigma^2$ ,  $E\{\eta_i(n)\} = 0$ , the noise is uncorrelated to the stimulus and

$$E\{\eta_i(n) * \eta_j(n)\} = 0, \quad i \neq j.$$

Then

$$x(n) = s(n) + \frac{1}{M} \sum_{i=1}^M \eta_i(n) = s(n) + \eta'(n).$$

The averaged noise signals variance  $\sigma_{\eta'}^2 = \sigma^2/M$ , and  $E\{\eta'(n)\} = 0$ . After the time averaging process the signal to noise ratio (SNR) improves

$$20 \lg(\sigma_{\eta}^2 / \sigma_{\eta'}^2) = 20 \lg(M) \text{ dB.}$$